Radiation Measurements 106 (2017) 140–145

Contents lists available at ScienceDirect

Radiation Measurements

journal homepage: www.elsevier.com/locate/radmeas

Development of BaF_2 transparent ceramics and evaluation of the scintillation properties

Takumi Kato [a, *], Go Okada [a], Kentaro Fukuda [b], Takayuki Yanagida [a]

[a] Graduate School of Materials Science, Nara Institute of Science and Technology (NAIST), 8916-5 Takayama-cho, Ikoma-shi, Nara 630-0192, Japan
[b] Tokuyama Corp., 1-1 Mikage-cho, Shunan-shi, Yamaguchi 745-8648, Japan

HIGHLIGHTS

- We have synthesized BaF_2 transparent ceramic by an SPS technique.
- We have characterized the optical, scintillation properties of BaF_2 transparent ceramic and single crystal.
- The scintillation light yield of the BaF_2 transparent ceramic was evaluated to be about 6000 photons/MeV under ^{137}Cs γ-rays.

ARTICLE INFO

Article history:
Received 12 September 2016
Received in revised form
21 March 2017
Accepted 22 March 2017
Available online 23 March 2017

Keywords:
Transparent ceramics
BaF_2
Scintillator
Dosimeter

ABSTRACT

We have developed BaF_2 transparent ceramics by using a spark plasma sintering (SPS), and investigated optical, scintillation and dosimeter properties, in comparison with a BaF_2 single crystal. The photoluminescence emission peak of transparent ceramics prepared in a vacuum condition appeared around 500 nm. Under X-ray irradiation, emissions at 190 and 220 nm due to auger-free luminescence (AFL) were observed in the ceramic samples. The scintillation light yield of the BaF_2 transparent ceramics was evaluated to be about 6000 photons/MeV under ^{137}Cs γ-rays. In addition, the afterglow level of ceramic sample was lower than that of the single crystal. Thermally-stimulated luminescence glow peaks were observed at 50, 105, 140, 205, 280 and 420 °C in all the samples.

1. Introduction

Inorganic scintillators, which convert high energy ionizing radiation to thousands of visible photons (Yanagida, 2013), have been playing a major role in many fields of radiation detection, including medical (Yanagida et al., 2010c), security (Totsuka et al., 2011), oil-logging (Yanagida et al., 2013b), environmental monitoring (Watanabe et al., 2015), astro- (Kokubun et al., 2004) and particle physics (Ito et al., 2007). In these applications, scintillators for γ-ray detections have attracted much attention especially for medical and security applications since these applications are very familiar to our daily life. Up to now, most scintillation detectors have consisted of single crystals mainly due to their high optical qualities. Except for Gd_2O_2S (Yoshida et al., 1988) used for X-ray CT and ZnS (McCloy et al., 2015) used for charged particle detectors, applications of ceramic materials are limited because the detection efficiency is generally restricted by the opacity of ceramics. However, thanks to the advancement of the ceramic technologies, we now have a new way to deform crystalline powder into a bulk ceramic in a transparent form, which has a great advantage to be used as a scintillator.

Barium fluoride (BaF_2) crystal is known as a potential scintillator material. In the 1970s, Farukhi and Swinehart (1971) have first reported scintillation by BaF_2 crystal due to auger-free luminescence (AFL) and self-trapped excitation (STE), which appear around 190–220 and 310 nm, respectively. In particular, BaF_2 has considerably large effective atomic number (Zeff = 52.7), so it has a great advantage to be used for γ-ray detections. However, compared with a conventional γ-ray scintillator ($Lu_{2-x}Y_xSiO_5$:Ce; 25,000 ph/MeV) used in PET, scintillation light yield of BaF_2 is much smaller (1500 ph/MeV). In addition, the emission spectral range of the AFL overlaps with that of STE, which has a much longer decay time constant (0.6 μs) (Blasse, 1994; Fedorov et al., 2016; Visser et al., 1993; Yanagida et al., 2010b). Most above studies have been performed using a single crystal form of BaF2; and there are large room

* Corresponding author.
E-mail address: kato.takumi.ki5@ms.naist.jp (T. Kato).

http://dx.doi.org/10.1016/j.radmeas.2017.03.032
1350-4487/

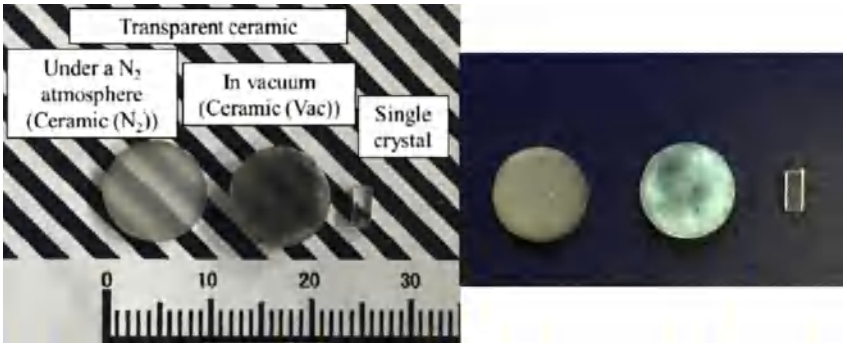

Fig. 1. BaF_2 ceramics and single crystal samples under room light (left) and UV (254 nm) light (right).

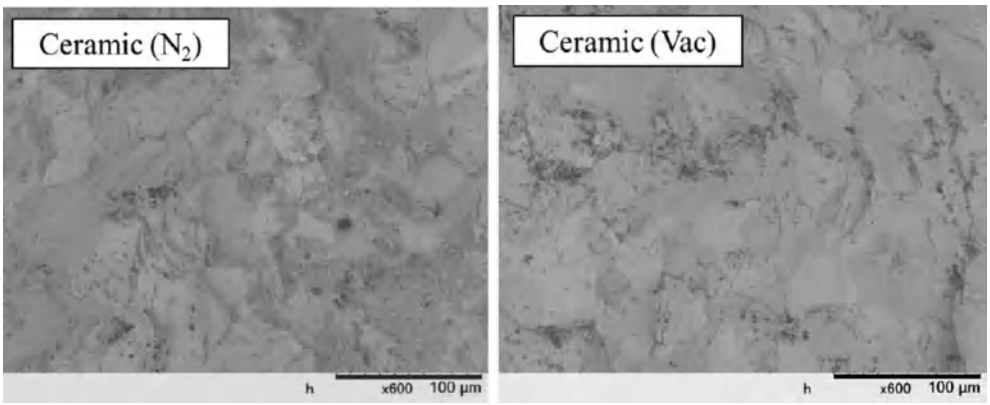

Fig. 2. SEM images of Ceramic (N_2) and (Vac).

for a development of BaF_2 transparent ceramics for scintillator applications. Earlier studies (Demidenko et al., 2010; Fedorov et al., 2016) have reported on non-doped and Ce-doped BaF_2 transparent ceramics; however, the scintillation in the vacuum-ultraviolet (VUV) range has not yet been evaluated and it has not been even known the scintillation in the VUV is present in a BaF_2 transparent ceramic, yet.

In this study, we developed the undoped BaF_2 transparent ceramics and characterized scintillation properties in relation with AFL. Specifically, the synthesis of BaF_2 transparent ceramics was carried out by the spark plasma sintering (SPS) method, and the optical and scintillation properties were characterized. Further, we have characterized the thermally stimulated luminescence (TSL) glow curve in order to study relatively shallow trapping centers. Up to now, our groups have succeeded to develop many kinds of transparent ceramic scintillators such as Ce:YAG (Yanagida et al., 2005), Ce:LuAG (Yanagida et al., 2011), Pr:LuAG (Yanagida et al., 2012), Ce:GAGG (Yanagida et al., 2013c) and Yb:Lu_2O_3 (Yanagida et al., 2013b). In these studies, most transparent ceramic samples showed superior scintillation properties than those of single crystals with the same chemical compositions; therefore, BaF_2 transparent ceramics are of great interest to investigate. In addition, to the best of our knowledge, no reports are found for bulk fluoride ceramics produced by SPS for scintillator applications.

2. Materials and methods

BaF_2 transparent ceramic samples were synthesized by the SPS method using Sinter Land LabX-100 as follows. First, BaF_2 powder (1.5 g) of a reagent grade was loaded in a graphite die and sealed with two graphite punches, and the graphite assembly was then

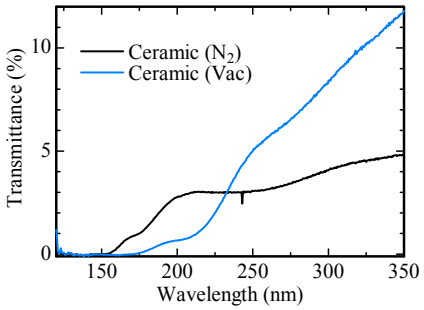

Fig. 3. Transmittance spectra of Ceramic (N_2) and Ceramic (Vac).

loaded to the furnace to sinter. The sintering temperature was controlled as described in the following sequence: the sintering temperature was increased from 20 °C to 720 °C at the rate of 24 °C/min and held for 30 min while applying the pressure of 10 MPa, and then the sintering temperature was increased to 960 °C at the rate of 24 °C/min and held for 45 min while applying the pressure of 100 MPa in a N_2 atmosphere or vacuum. In this paper, we denote the obtained samples Ceramic (N_2) and Ceramic (Vac) for the ones sintered in N_2 and vacuum, respectively. After the synthesis, the wide surfaces of the ceramic samples were polished. In the course of study, the following measurements were carried out for all the prepared samples, and some of the measurements were done for BaF2 single crystal prepared by Tokuyama Corp. In these experiments, all the ceramics and the reference single crystals were synthesized by using the same BaF_2 powders.

Backscattered electron image of ceramic sample was obtained

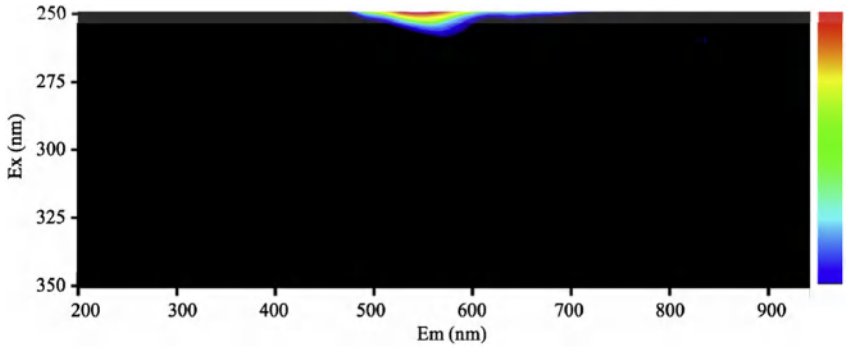

Fig. 4. PL excitation and emission map of Ceramic (Vac).

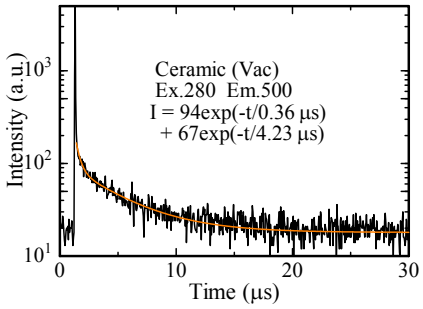

Fig. 5. PL decay profile of Ceramic (Vac). The monitoring PL emission wavelength is 500 nm under the excitation at 280 nm.

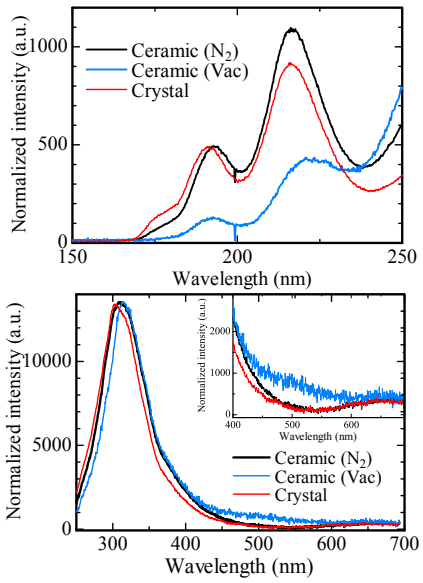

Fig. 6. X-ray induced scintillation spectra of all the samples in the VUV-UV (up) and UV-VIS (bottom) spectral regions. The inset of right figure is expand 400–650 nm.

by using scanning electron microscope (SEM; Hitachi TM3030). SEM images were observed on a fractured surface. The transmittance spectrum from 100 to 350 nm was measured by Tokuyama Corp. The PL excitation and emission map was measured by using Quantaurus-QY (C11347-01, Hamamatsu Photonics). The PL decay lifetime monitoring at 500 nm was observed under 280 nm excitation using Hamamatsu Quantaurus-τ (C11367-04, Hamamatsu). The 280 nm excitation is the shortest wavelength of LED equipped to Hamamatsu Quantaurus-τ. In this paper, we do not report these optical properties of BaF2 single crystal since many literature have already discussed.

The X-ray induced scintillation spectrum from 250 to 700 nm was measured by using our lab-constructed setup. The sample was excited using an X-ray generator in which the applied tube voltage and current were 40 kV and 5.2 mA, respectively. The scintillation emission was guided to Ocean Optics CCD-based spectrometer (QEPro). The details of the setup was described previously (Yanagida et al., 2013c). The X-ray induced scintillation spectrum in the VUV-UV region (150–250 nm) was measured by using a custom-made setup described in the literature (Abe et al., 2010). Further, the scintillation lifetime was evaluated by the pulse X-ray equipped streak camera system. In this measurement, we set the monitoring wavelength at 190–220 nm to observe AFL (Fujimoto et al., 2011; Furuya et al., 2011; Yanagida et al., 2010a). In order to evaluate scintillation decay times of STE, we used an afterglow characterization system equipped with a pulse X-ray tube (Yanagida et al., 2014). Furthermore, to investigate the amount of defects qualitatively, afterglow profiles by X-ray irradiation was measured using also the afterglow characterization system.

In the pulse height measurement, we mounted a sample piece on the window of PMT (R8778, Hamamatsu) with a silicon grease (6262A, OKEN), and the sample was covered by several layers of Teflon reflectors to guide scintillation photons to the photoelectric converter of the PMT. When γ–rays from ^{137}Cs was detected by the sample, the scintillation photons are converted to electronic signal by the PMT, which is then processed by the preamplifier (113, ORTEC), shaping-amplifier (572, ORTEC) with 0.5 μs shaping time and multichannel analyzer (AMPTEK Pocket MCA). The pulse height spectrum is eventually stored on a computer.

In order to characterize relatively shallow trapping centers, we have measured a TSL glow curve using a Nanogray TL-2000 (Yanagida et al., 2013a) after X-ray irradiations with 10 Gy. The heating rate used for all the TSL measurements was fixed to 1 °C/s, and the sample was heated from 50 to 490 °C to measure the glow curve.

3. Results and discussion

Fig. 1 illustrates the synthesized BaF_2 transparent ceramic and single crystal samples. The single crystal sample was prepared by Tokuyama Corp. The left photograph shows the samples under the room light while the right image shows those under UV (254 nm) light. Both the prepared ceramic samples are visually transparent. The Ceramic (Vac) sample showed a green emission under UV light as shown in the right figure. Fig. 2 depicts SEM images of Ceramic (N_2) and Ceramic (Vac). From the SEM images, it can be confirmed that the ceramic samples were highly densified and properly

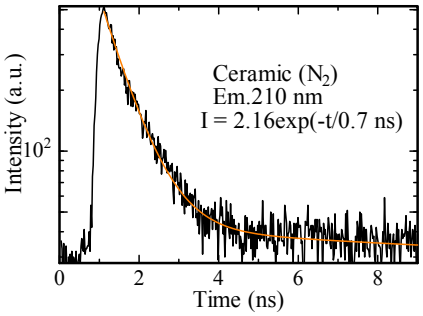

Fig. 7. Scintillation decay profile of Ceramic (N_2) monitoring wavelength at 190–220 nm.

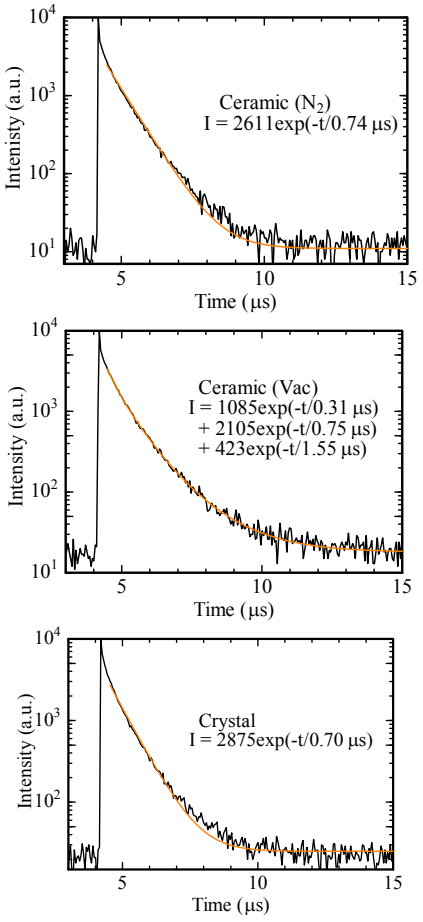

Fig. 8. Scintillation decay profiles of Ceramic (N_2), Ceramic (Vac) and crystal monitoring wavelength at 300–650 nm.

sintered. In these samples, a typical grain diameters of the Ceramic (N_2) and Ceramic (Vac) samples are estimated to be about 35 and 30 μm, respectively.

Fig. 3 shows transmittance spectra of Ceramic (N_2) and Ceramic (Vac). Both the ceramic samples showed detectable transmittance signal at the wavelengths as short as approximately 150 nm. Although the transmittance is inferior to that of commercial BaF_2 single crystal, optical absorption edge is equivalent. Thus, optical transparency in the UVU region is also achievable in a transparent ceramic form.

The PL excitation and emission map of Ceramic (Vac) is represented in Fig. 4. The measured excitation range was in the near ultraviolet (UV) while the emission range was in the UV, visible and near infrared (NIR) regions. Among all the samples measured, we could only detect PL emission by the Ceramic (Vac) which appear around 500 nm under 250 nm excitation. From the spectral bandwidth, the origin of this emission seems to be attributable to d-f transitions of rare earths, d-d transitions of transition metals or some kinds of defects. The PL quantum yield of this green emission was 2.5%.

The PL decay profiles of Ceramic (Vac) is shown in Fig. 5. Subsequently, measured PL decay curve for 500 nm peak was approximated by a sum of two exponential decay functions, and the obtained decay time constants were 0.36 and 4.23 μs? From these values, it is conceivable that the 500 nm peak was due to the d-f transitions of Eu^{2+} ions. However, the d-f transitions of divalent rare earth ions were impossible in BaF_2 because the excited 5d states of RE^{2+} lie in the conduction band of the BaF_2 crystal (Rodnyi et al., 2007); therefore, the possibilities of rare earths and transition metals which show typically decay time on an order of ms were dismissed. Because the excitation bands of this green emission appeared within the bandgap (~250 nm), the possible origin would be some kinds of defects.

Fig. 6 indicates the scintillation spectra of all the samples in the VUV-UV (left) and UV-VIS (right) spectral regions. When X-ray was irradiated, all the samples showed an emission at 320 nm due to the STE luminescence. Moreover, in Ceramic (Vac), another peak appeared at 500 nm, and this emission wavelength was consistent with that in PL. The presence of emission at 500 nm has not been reported in previous studies for undoped BaF_2 single crystals and ceramics (Abe et al., 2010; Farukhi and Swinehart, 1971; Hamada et al., 1994). Supported by the PL analyses, we consider that this emission is attributed to some kinds of defects generated during the sintering processes by the SPS. Since this emission is not present in the sample sintered in N_2 atmosphere, the emission origin would be anion vacancies. Subsequently, we measured scintillation spectra of ceramic samples in VUV range, and emission peaks were detected at 190 and 220 nm, which are due to the AFL. The presence of both AFL and STE emission confirms that our ceramic samples have a good crystalline quality at least in the each grain scale. In the Ceramic (Vac), the emission intensity of AFL was smaller than that of the Ceramic (N_2) although the sample size was comparable. So, the presence of defects may suppress AFL.

The X-ray induced scintillation decay profile of Ceramic (N_2) monitoring at 190–220 nm is shown in Fig. 7. The observed decay constant was 0.69 ns, and the value is consistent with the reported value for single crystal (Demidenko et al., 2010). In Ceramic (Vac), we could not detect the decay component due to AFL because of low scintillation intensity. Fig. 8 demonstrates the scintillation decay profiles of Ceramic (N_2), Ceramic (Vac) and crystal monitoring at 300–650 nm, and measured decay time constants are summarized in Table 1. The scintillation decay time constants for 500 nm of Ceramic (Vac) were 0.31 and 1.55 μs, and which were approximately the same as those measured in PL. Moreover, the decay time constant due to the STE of Ceramic (N_2), Ceramic (Vac) and crystal samples were 0.74, 0.75 and 0.70 μs, respectively (Demidenko et al., 2010).

Table 1
Scintillation decay time constants.

	Scintillation decay time constant		
	AFL (ns)	STE (μs)	Green emission (μs)
Ceramic (N_2)	0.69	0.74	–
Ceramic (Vac)	–	0.75	0.31, 1.55
Crystal	0.70	0.70	–

Fig. 9 demonstrates afterglow profiles after an X-ray irradiation with a pulse duration of 2 ms. Afterglow levels of Ceramic (N_2), Ceramic (Vac) and crystal are 0.0112, 0.0004 and 0.0153%, and Ceramic (Vac) shows the lowest afterglow level among the present samples. From this result, it can be said that afterglow levels of transparent ceramics are improved in comparison with the one of single crystal although many grain boundaries are created in ceramics. In this evaluation, afterglow levels (A) are represented A (%) = 100 × (I_2–I_0)/(I_1–I_0) where I_0, I_1 and I_2 denote the averaged background signal, the averaged signal intensity during X-ray irradiation and signal intensity at 20 ms after the X-ray irradiation, respectively. We referred the formula from the evaluation manner of NIHON KESSHO KOGAKU CO., LTD. which is one of the well-known manufactures of scintillation detectors for medical and security applications.

Pulse height spectra of all samples measured under ^{137}Cs exposure are shown in Fig. 10. Clear photoabsorption peaks were detected in Ceramic (N_2) and crystal samples while no photoabsorption peak was detected in Ceramic (Vac). The absolute light yield of Ceramic (N_2) was determined as 6000 ph/MeV. From this result, it was found that green emission act as negative for scintillation. Although the light yield is inferior to the single crystal in this time, the light yield would be improved when the synthesis methods and conditions are optimized as same as the cases of transparent ceramic garnet scintillators. The important thing in this work is that we can prepare bulk transparent ceramic BaF_2, and this ceramic sample can show AFL and significant transmittance in VUV wavelength.

Fig. 11 shows TSL glow curves measured after samples were irradiated with an X-ray dose of 10 Gy. The glow curves were decomposed by Gaussian functions. In this analysis, we fixed the number of peaks and peak positions according to previous reports on BaF_2 single crystal (Drozdowski et al., 1999; Sabharwal et al., 2002), and the peak width was free during the deconvolution. The Gaussian component located at the highest temperature was

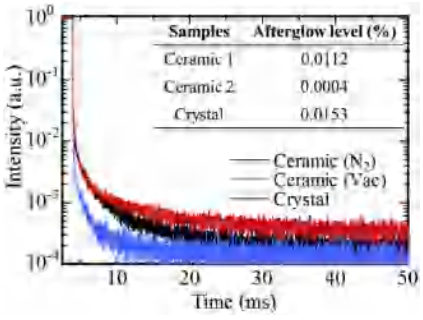

Fig. 9. Afterglow profiles of Ceramic (N_2), Ceramic (Vac) and Crystal.

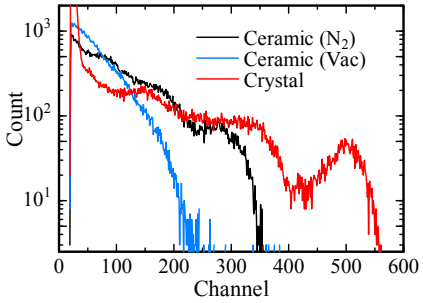

Fig. 10. Pulse height spectra measured under ^{137}Cs γ-ray irradiation.

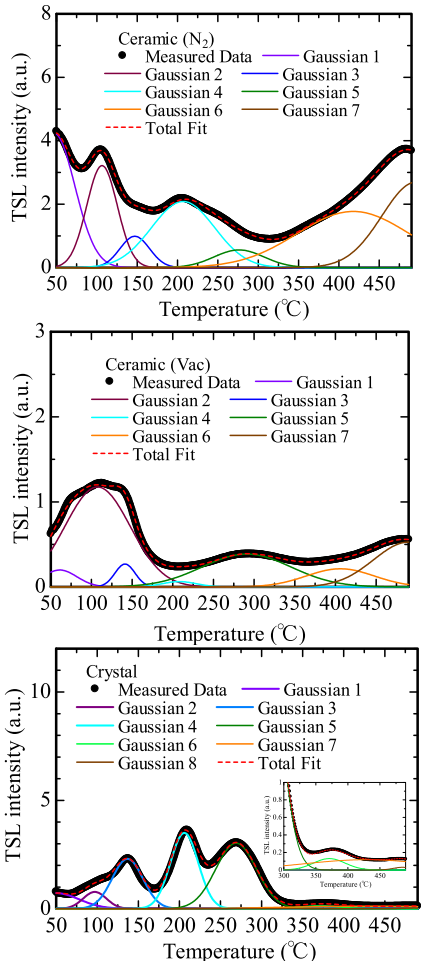

Fig. 11. TSL glow curves of all samples after X-ray irradiation 10 Gy. The inset shows the enlarged view from 300 to 490 °C.

treated as a contribution of black-body radiation by the heater. For both Ceramic (N_2) and Ceramic (Vac), there appeared six TSL glow peaks centered at 50, 105, 140, 205, 280 and 420 °C. In addition, a TSL glow peak of the single crystal sample appeared at 380 °C. Since there is no differences between the glow peak temperatures of the two ceramic samples, the possible anion defects present in Ceramic (N_2) (which act as luminescent center to show green broad emission) may not affect the energy storage process. The glow peak at 380 °C was only observed in the crystal sample, so it should be due to some trapping centers specifically created during crystal synthesis processes. Judging from the glow intensity, the amount of defects acting as trapping center in Ceramic (N_2) is the largest among the present samples. Improvement of scintillation properties is expected by reducing the amount of defects because dosimeter properties have complementarity to scintillation properties.

4. Conclusion

We have developed BaF_2 transparent ceramics by the SPS method under N_2 and vacuum environments and then investigated the optical, scintillation and TSL properties, in comparison with BaF_2 single crystal. Emissions by the STE and AFL were observed for both the ceramic samples as well as the crystal sample. The scintillation light yield of the ceramic sample sintered in a N_2 atmosphere was approximately 6000 photons/MeV, and this value was

smaller than that of the single crystal. In addition, the afterglow levels of ceramic samples were better than that of the single crystal. However, TSL intensity of ceramic samples were much stronger than the single crystal sample.

Acknowledgement

This work was supported by a Grant in Aid for Scientific Research (A)-26249147 from the Ministry of Education, Culture, Sports, Science and Technology of the Japanese government (MEXT) and partially by JST A-step. The Cooperative Research Project of Research Institute of Electronics, Shizuoka University, KRF foundation, Hitachi Metals Materials Science foundation, and Inamori Foundation are also acknowledged.

References

Abe, N., Yokota, Y., Yanagida, T., Pejchal, J., Nara, F., Kawaguchi, N., Fukuda, K., Nikl, M., Yoshikawa, A., 2010. Crystal growth and luminescence properties of Tm:BaF_2 single crystals. Jpn. J. Appl. Phys. 49, 022601.

Blasse, G., 1994. Scintillator materials. Chem. Mater 6, 1465–1475.

Demidenko, A.A., Garbin, S.D., Gusev, Y.I., Fedorov, P.P., Mironov, I.A., Michrin, S.B., Osiko, V.V., Rodnyi, P.A., Seliverstov, D.M., Smimov, A.N., 2010. Scintillation parameters of BaF_2 and BaF_2:Ce^{3+} ceramics. Opt. Mat. 32, 1291–1293.

Drozdowski, W., Przegietka, K.R., Wojtowicz, A.J., Oczkowski, H.L., 1999. Charge traps in Ce-doped CaF_2 and BaF_2. A. Cta. Phys. Pol. A 95, 251–258.

Farukhi, M.R., Swinehart, C.F., 1971. Barium fluoride as a gamma ray and charged particle detector. IEEE Trans. Nucl. Sci. 18, 200–204.

Fedorov, P.P., Ashurov, M.K., Boboyarova, S.G., Boibobeva, S., Nuritdinov, I., Garibin, E.A., Kuznetsov, S.V., Smirnov, A.N., 2016. Absorption and luminescence spectra of CeF_3-doped BaF_2 single crystals and nanoceramics. Inorg. Mater 52, 213–217.

Fujimoto, Y., Yanagida, T., Sekiwa, H., Yokota, Y., Yoshikawa, A., 2011. Scintillation characteristic of in,Ga-doped ZnO thin films with different dopant concentrations. Jpn. J. Appl. Phys. 50, 01BG04.

Furuya, Y., Yanagida, T., Fujimoto, Y., Yokota, Y., Kamada, K., Kawaguchi, N., Ishizu, S., Uchiyama, K., Mori, K., Kitano, K., Nikl, M., Yoshikawa, A., 2011. Time- and wavelength-resolved luminescence evaluation of several types of scintillators using streak camera system equipped with pulsed X-ray source, 2011. Nucl. Instrum. Methods Phys. Res. A 634, 59-63 Nucl. Instrum. Methods Phys. Res. A 634, 59–63.

Hamada, M.M., Nunoya, Y., Sakuragui, S., Kubota, S., 1994. Suppression of the slow component of BaF_2 crystal by introduction of SrF_2 and MgF_2 crystals. Nucl. Instrum. Methods 353, 33–36.

Ito, T., Yanagida, T., Sato, M., Kokubun, M., Takashima, T., Hirakuri, S., Miyawaki, R., Takahashi, H., Makishima, K., Tanaka, T., Nakazawa, K., Takahashi, T., Honda, T., 2007. A1-dimensional γ-ray position sensor based on GSO: Ce scintillators coupled to a Si strip detector. Nucl. Instr. Meth. A 579, 239–242.

Kokubun, M., Abe, K., Ezoe, Y., Fukazawa, Y., Hong, S., Inoue, H., Itoh, T., Kamae, T., Kasama, D., Kawaharada, M., Kawano, N., Kawashima, K., Kawasoe, S., Kobayashi, Y., Kotoku, J., Kouda, M., Kubota, A., Madejski, G.,M., Makishima, K., Mitani, T., Miyasaka, H., Miyawaki, R., Mori, K., Mori, M., Murakami, T., Murashima, M.,M., Nakazawa, K., Niko, H., Nomachi, M., Ohno, M., Okada, Y., Oonuki, K., Sato, G., Suzuki, M., Takahashi, H., Takahashi, I., Takahashi, T., Tamura, K., Tanaka, T., Tashiro, M., Terada, Y., Tominaga, S., Watanabe, S., Yamaoka, K., Yanagida, T., Yonetoku, D., 2004. Improvements of the astro-E2 hard X-ray detector (HXD-II). IEEE Trans. Nucl. Sci. 51, 1991–1996.

McCloy, J.S., Bliss, M., Miller, B., Wang, Z., Stave, S., 2015. Scintillation and luminescence in transparent colorless single and polycrystalline bulk ceramic ZnS. J. Lumin 157, 416–423.

Rodnyi, P.A., Khodyuk, I.V., Stryganyuk, G.B., 2007. Location of the energy levels of the rare-earth ions in BaF_2 and CdF_2. Phys. Solid. State 50, 1639–1643.

Sabharwal, S.C., Sangeeta, Chauhan, A.K., 2002. Effect of lattice oxygen on optical absorption, radiation hardness and thermally stimulated luminescence of BaF_2 crystal. J. Cryst. Growth 240, 473–478.

Totsuka, D., Yanagida, T., Fukuda, K., Kawaguchi, N., Fujimoto, Y., Yokota, Y., Yoshikawa, A., 2011. Performance test of Si PIN photodiode line scanner for thermal neutron detection. Nucl. Instrum. Methods A 659, 399–402.

Visser, R., Dorenbos, P., Andriessen, J., Eijk, C.W.E., 1993. Scintillation properties and mechanisms of Ce and La doped BaF_2 crystals. Nucl. Tracks. Rad. Meas. 21, 201–204.

Watanabe, K., Yanagida, T., Fukuda, K., Koike, A., Aoki, T., Uritani, A., 2015. Portable neutron detector using Ce:$LiCaAlF_6$ scintillator. Sensors Mater. 27 (3), 269–275.

Yanagida, T., Takahashi, H., Ito, T., Kasama, D., Enoto, T., Sato, M., Hirakuri, S., Kokubun, M., Makishima, K., Yanagitani, T., Yagi, H., Shigeta, T., Ito, T., 2005. Evaluation of properties of YAG (Ce) ceramic scintillators. IEEE. Nucl. Trans. Sci. 52, 1836–1841.

Yanagida, T., Fujimoto, Y., Yoshikawa, A., Yokota, Y., Kamada, K., Pejchal, J., Kawaguchi, N., Fukuda, K., Uchiyama, K., Mori, K., Kitano, K., Nikl, M., 2010a. Development and performance test of picosecond pulse X-ray excited streak camera system for scintillator characterization. Appl. Phys. Express 3, 056202.

Yanagida, T., Kawaguchi, N., Yokota, Y., Ishidu, S., Fukuda, K., Yoshikawa, A., Pejchal, J., Nikl, M., Babin, V., Sekiya, H., Kamada, K., 2010b. Study of VUV emission and g-ray responses of Nd:BaF_2 scintillaotor. Radiat. Meas. 45, 422–425.

Yanagida, T., Yoshikawa, A., Yokota, Y., Kamada, K., Usuki, Y., Yamamoto, S., Miyake, M., Baba, M., Sasaki, K., Ito, M., 2010c. Development of Pr:LuAG scintillator array and assembly for positron emission mammography. IEEE Trans. Nucl. Sci. 57, 1492–1495.

Yanagida, T., Fujimoto, Y., Yokota, Y., Kamada, K., Yanagida, S., Yoshikawa, A., Yagi, H., Yanagitani, T., 2011. Comparative study of transparent ceramic and single crystal Ce doped LuAG scintillators. Rad. Meas. 46, 1503–1505.

Yanagida, T., Fujimoto, Y., Kamada, K., Totsuka, D., Yagi, H., Yanagitani, T., Futami, Y., Yanagida, S., Kurosawa, S., Yokota, Y., Yoshikawa, A., Nikl, M., 2012. Scintillation properties of transparent ceramic Pr:LuAG for different Pr concentration. IEEE Trans. Nucl. Sci. 59, 2146–2151.

Yanagida, T., 2013. Study of rare-earth-doped scintillators. Opt. mater 35, 1987–1992.

Yanagida, T., Fujimoto, Y., Kawaguchi, N., Yanagida, S., 2013a. Dosimeter properties of AlN. J. Ceram. Soc. Jpn. 121, 988–991.

Yanagida, T., Fujimoto, Y., Kurosawa, S., Kamada, K., Takahashi, H., Fukazawa, Y., Nikl, M., Chani, V., 2013b. Temperature dependence of scintillation properties of bright oxide scintillators for well-logging. Jpn. J. Appl. Phys. 52, 076401.

Yanagida, T., Kamada, K., Fujimoto, Y., Yagi, H., Yanagitani, T., 2013c. Comparative study of ceramic and single crystal Ce:GAGG scintillator. Opt. Mater 35, 2480–2485.

Yanagida, T., Fujimoto, Y., Ito, T., Uchiyama, K., Mori, K., 2014. Development of X-rays-induced afterglow characterization system. Appl. Phys. Exp. 7, 062401.

Yoshida, M., Nakagawa, M., Fujii, H., Kawaguchi, F., Yamada, H., Ito, Y., Takeuchi, H., Yayakawa, T., Tsukuda, Y., 1988. Application of Gd2O2S ceramic scintillator for X-ray solid state detector in X-ray CT. Jpn. J. Appl. Phys. 27, 1572–1575.